

Anomalous Stability of Carbon Dioxide in pH-Controlled Bubble Coalescence**

Rico F. Tabor, Derek Y. C. Chan, Franz Grieser, and Raymond R. Dagastine*

Gas bubbles are formed as cavities in liquids, their pressure, shape, and deformability determined by the surface tension of the liquid. They are vital components in foams, microfluidics,^[1] sonochemical reactions,^[2] generation of atmospheric aerosol,^[3] and in the scent and taste delivery of soft drinks, beers, and champagne.^[4] In all of these cases, their stability or coalescence during inter-bubble collisions is a vital factor in determining bubble behavior and lifetime. It has been noted previously that, due to its high water-solubility and unusual aqueous chemistry, carbon dioxide may be expected to behave differently than inert gases,^[5] suggesting that a comparative study is needed. Here, we explore bubble coalescence as a function of pH and gas type, demonstrating that CO₂ has a surprising and vital role, by comparing pure CO₂ bubbles with air (which has CO₂ as a minor component), argon, and nitrogen (pure, inert gases).

Recently, advances in the technique of atomic force microscopy (AFM) have allowed direct measurements of the force and coalescence behavior between pairs of bubbles and drops with diameters around 100 μm to be made.^[6–8] Here, for the first time we use low velocities in order to understand the equilibrium forces acting between bubbles as they approach one another, and which ultimately determine their coalescence or stability.

Bubble interaction events were measured by using an AFM cantilever to pick one bubble up in the size range 50–200 μm from a glass substrate, and drive this bubble towards a substrate-immobilized bubble at a fixed, low speed (0.2 μm s⁻¹, chosen to eliminate the effects of hydrodynamic drainage forces between the bubbles), until either coalescence occurred, or until a fixed deflection of the cantilever

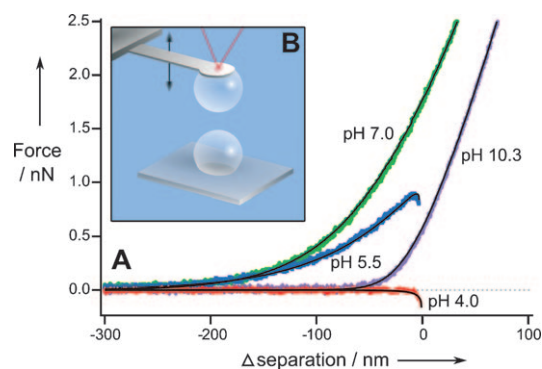


Figure 1. A) Force vs. relative separation curves for the slow (0.2 μm s⁻¹) approach of two air bubbles in different pH conditions. At pH 7 and 10.3, stable interactions are observed; for pH 4 and 5.5, coalescence occurs. Colored points are the experimental data, and solid black lines are the model prediction. Δseparation is defined as the change in separation between the end of the cantilever and the solid surface. B) Schematic of the AFM experiment, showing a bubble attached to the cantilever approaching a surface-immobilized bubble.

was reached in the case of stable, repulsive interactions. The experiment is shown schematically in Figure 1B, and full details of experimental procedures used are included in the Supporting Information.

During the axisymmetrical, close approach of two bubbles (Figure 1), they will deform and flatten in the presence of a repulsive interaction and a film of water will remain between the two air–water interfaces.^[7,8] The thickness of this film depends on the disjoining pressure which includes contributions from van der Waals and electrical double-layer interactions. By using a theoretical model^[8–10] (included in the Supporting Information) that couples a quantitative description of these forces to expressions that describe the interfacial profiles of the bubbles during an AFM measurement, information on both the surface forces and deformation can be calculated.

The pH ranges investigated for each gas, and the regions in which coalescence were observed are shown in Figure 2. For the inert gases, argon and nitrogen, the window of coalescence is almost identical, between pH 3 and 7. For air, this region is smaller by half a pH unit at each extreme. In contrast, CO₂ bubbles do not coalesce below pH 6, showing considerably enhanced stability.

Surface potentials derived from model fits to the data as a function of pH for the gas bubbles are presented in Figure 3. It is found that the surface potentials for air bubbles are in general agreement with those obtained using microelectrophoresis,^[11] including the location of the isoelectric point close to pH 4. For argon and nitrogen bubbles, the surface

[*] Dr. R. F. Tabor, Prof. R. R. Dagastine
Department of Chemical and Biomolecular Engineering
University of Melbourne, Parkville 3010 (Australia)
Fax: (+61) 3-8344-4153
E-mail: rrd@unimelb.edu.au
Homepage: <http://www.chemeng.unimelb.edu.au/people/staff/dagastine.html>

Prof. D. Y. C. Chan
Department of Mathematics and Statistics
University of Melbourne, Parkville 3010 (Australia)

Prof. F. Grieser
School of Chemistry, University of Melbourne
Parkville 3010 (Australia)

[**] We thank G. W. Stevens, T. Raymond, and L. Paterson for comments and discussions. X. S. Tang and S. O'Shea are thanked for preparing the cantilevers used. The ARC is thanked for financial support. The PFPC is thanked for providing infrastructure support for the project

Supporting information for this article is available on the WWW under <http://dx.doi.org/10.1002/anie.201006552>.

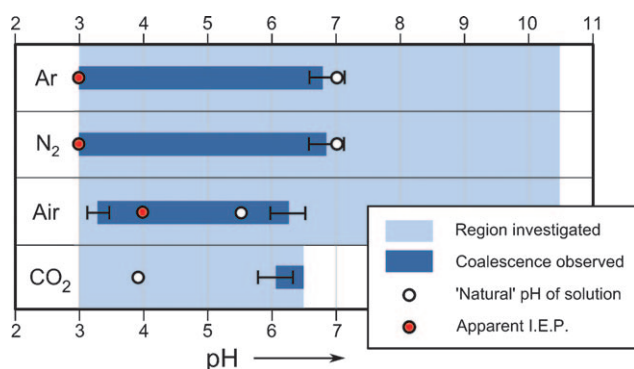


Figure 2. The observed windows of bubble coalescence for four gases over the pH ranges tested. CO₂ bubbles could not be easily generated above pH 6.5 due to the high gas solubility. The “natural” pH is the unadjusted pH of the saturated gas in water. The error bars denote the confidence in the boundaries of the coalescence region.

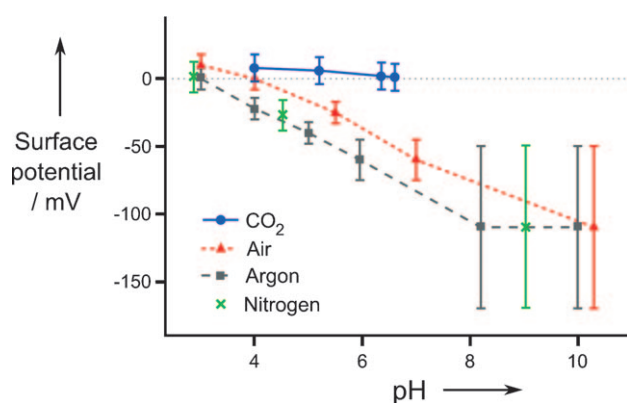


Figure 3. Surface potentials for the different gas bubbles as a function of pH. For air, argon, and nitrogen these are derived from fits to the approach force curves for two bubbles. For CO₂, they are from fits of the approach of a bubble towards a flat alumina plate (see Supporting Information). The error bars reflect the sensitivity of the measurement, and lines have been drawn to guide the eye.

potentials are shifted down by approximately one pH unit to be more acidic, with an isoelectric point at around pH 3, also in agreement with literature values for inert gases.^[12]

For argon, nitrogen, and air the primary mechanism for stabilization of bubbles can be explained by electrical double-layer repulsion, due to adsorbed charged groups. At low pH (for air) it has been suggested that these species are protons,^[11] whereas at higher pH, adsorption of hydroxide ions is the accepted mechanism.^[13,14] Beattie et al. pointed out that the surface of “neat” water is basic due to adsorption of hydroxide ions,^[12,14] which are recognized to stabilize both bubbles and emulsion droplets.^[15]

For pH values close to the isoelectric point, the effect of electrostatics is too small to prevent bubbles from approaching sufficiently closely to allow the short-range van der Waals attraction to take over and induce coalescence (Figure 1). For air bubbles, at pH 5.5, a weak repulsive maximum due to electrostatic repulsion is evident before the short-range van der Waals force induces coalescence. At pH 4, the apparent isoelectric point (IEP), there is no evidence of surface charge,

and the only force is attributed to a van der Waals attraction. For pH values outside of the window of coalescence, the electrical double-layer repulsion is sufficient such that the film never becomes thin enough to access a region where the van der Waals attraction overcomes the double-layer repulsion, and hence coalescence does not occur.

When dissolved in water, CO₂ establishes complex chemical equilibria involving the solvated gas, carbonic acid (H₂CO₃), dissociated protons, and bicarbonate (HCO₃⁻) ions, and the speciation of CO₂ as a function of pH is shown in Figure 4C. It has been noted previously that CO₂ and its

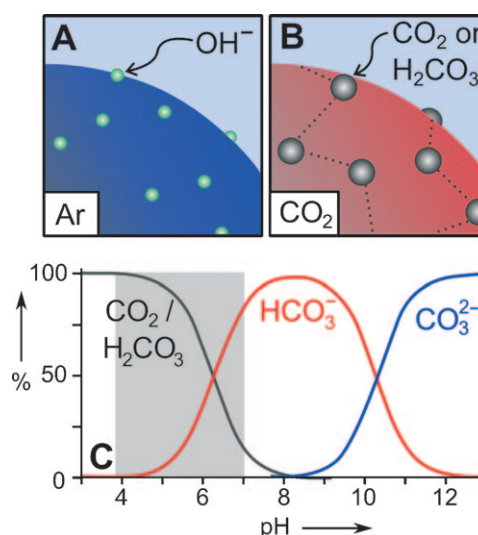


Figure 4. A) The suggested adsorption on an inert gas bubble (no CO₂ present) at pH > 4. B) The suggested adsorption of carbonic acid on a CO₂ bubble at pH 4–6. The dashed lines represent likely hydrogen.

solution species adsorb at the air–water interface,^[5,16] supported by the observation that the surface tension of CO₂–water is lower than that of air–water or inert gas–water.^[16,17] The high-force region of the force interaction data between CO₂ bubbles in this work agrees with this result, suggesting a water–CO₂ interfacial tension of 65 mN m⁻¹. It is suggested here that these adsorbed species may displace hydroxide ions from the bubble surfaces, explaining the shift of the IEP when comparing argon, air, and pure CO₂ (Figure 4B). Additionally, this adsorbed “foliage” may contribute steric repulsion at close approach of CO₂ bubbles, explaining their anomalous stability. This is further supported by the narrower window of coalescence for air when compared to argon and nitrogen. As base is added to adjust the solution pH to higher values, dissolved CO₂ and carbonic acid decrease sharply in concentration. This appears to eventually cause instability of CO₂ bubbles, seen above pH 6. As the solubility of CO₂ in water increases so significantly with pH, after pH 6.5, it was no longer possible to generate bubbles.

Although the surface charge of water has been a subject of research for many decades,^[13,18] there has been considerable renewed interest in the topic recently: computer simulations suggest that the air–water interface should bear a net positive charge,^[19] whereas experiments show the opposite behav-

ior.^[14] The present work is not only consistent with previous experimental observations, but demonstrates that the charging behavior of the air–water interface is dependent on the presence of CO₂ and on the pH, which are clearly linked through acidic speciation of CO₂ in solution. The results may offer some insight and give caution to comparisons between experimental observations and computer simulations that do not account for CO₂ speciation.

As a whole, these results demonstrate that bubble coalescence in water is highly dependent on gas type and pH. The speciation equilibria from dissolved carbon dioxide play an important role, whether CO₂ is present as a pure gas, or as a minority component (for the case of air), and suggest that measurements of the surface of water should include the possibility of CO₂ species as a surface-active component.

Received: October 19, 2010

Revised: December 17, 2010

Published online: March 11, 2011

Keywords: adsorption · bubbles · carbon dioxide · interfaces · surface potential

[1] M. Prakash, N. Gershenfeld, *Science* **2007**, *315*, 832–835.

[2] M. Ashokkumar, F. Grieser, *Rev. Chem. Eng.* **1999**, *15*, 41–83.

[3] C. D. O'Dowd, G. de Leeuw, *Philos. Trans. R. Soc. London Ser. A* **2007**, *365*, 1753–1774.

[4] G. Liger-Belair, C. Cilindre, R. D. Gougeon, M. Lucio, I. Gebefügi, P. Jeandet, P. Schmitt-Kopplin, *Proc. Natl. Acad. Sci. USA* **2009**, *106*, 16545–16549.

[5] J. F. Harper, *J. Fluid Mech.* **2007**, *581*, 157–165.

[6] O. Manor, I. U. Vakarelski, X. Tang, S. J. O'Shea, G. W. Stevens, F. Grieser, R. R. Dagastine, D. Y. C. Chan, *Phys. Rev. Lett.* **2008**, *101*, 024501.

[7] I. U. Vakarelski, R. Manica, X. Tang, S. J. O'Shea, G. W. Stevens, F. Grieser, R. R. Dagastine, D. Y. C. Chan, *Proc. Natl. Acad. Sci. USA* **2010**, *107*, 11177–11182.

[8] R. R. Dagastine, R. Manica, S. L. Carnie, D. Y. C. Chan, G. W. Stevens, F. Grieser, *Science* **2006**, *313*, 210–213.

[9] R. Manica, J. N. Connor, R. R. Dagastine, S. L. Carnie, R. G. Horn, D. Y. C. Chan, *Phys. Fluids* **2008**, *20*, 032101.

[10] R. R. Dagastine, L. R. White, *J. Colloid Interface Sci.* **2002**, *247*, 310–320.

[11] M. Takahashi, *J. Phys. Chem. B* **2005**, *109*, 21858–21864.

[12] P. Creux, J. Lachaise, A. Graciaa, J. K. Beattie, A. M. Djerdjev, *J. Phys. Chem. B* **2009**, *113*, 14146–14150.

[13] C. Stubenrauch, R. von Klitzing, *J. Phys. Condens. Matter* **2003**, *15*, R1197–R1232.

[14] J. K. Beattie, A. M. Djerdjev, G. G. Warr, *Faraday Discuss.* **2009**, *141*, 31–39.

[15] J. K. Beattie, A. M. Djerdjev, *Angew. Chem.* **2004**, *116*, 3652–3655; *Angew. Chem. Int. Ed.* **2004**, *43*, 3568–3571.

[16] R. Massoudi, A. D. King, *J. Phys. Chem.* **1974**, *78*, 2262–2266.

[17] W. Yan, G.-Y. Zhao, G.-J. Chen, T.-M. Guo, *J. Chem. Eng. Data* **2001**, *46*, 1544–1548.

[18] H. A. McTaggart, *Philos. Mag.* **1914**, *27*, 297–299.

[19] V. Buch, A. Milet, R. Vacha, P. Jungwirth, J. P. Devlin, *Proc. Natl. Acad. Sci. USA* **2007**, *104*, 7342–7347.